Available online at www.sciencedirect.com
ScienceDirect
Journal of Catalysis 244 (2006) 219–229
JOURNAL OF CATALYSIS
www.elsevier.com/locate/jcat

Synthesis of dimethyl carbonate and dimethoxy methane over Cu-ZSM-5

Yihua Zhang, Ian J. Drake, Daniel N. Briggs, Alexis T. Bell *

Department of Chemical Engineering, University of California, Berkeley, CA 94720, USA

Received 18 June 2006; revised 23 August 2006; accepted 1 September 2006

Available online 12 October 2006

Abstract

An investigation was carried out of the oxidative carbonylation of methanol to dimethyl carbonate over Cu-ZSM-5. The catalyst was prepared by solid-state ion exchange of H-ZSM-5 with CuCl and then characterized by X-ray absorption spectra (XAS). The XANES portion of the XAS data showed that all of the copper is present as Cu^+ cations, and analysis of the EXAFS portion of the data shows the Cu^+ cations have a Cu-O coordination number of ∼2.7, suggesting that the cations are doubly and triply coordinated. Under DMC synthesis conditions, cuprous cations can be identified by two sorts of sites, one site covered by methanol only and a second on which CO and methanol co-absorb. In the absence of CO, DMM is the primary product formed, but when CO is present DMC becomes the primary products. DMM and MF are presumed to form via the coupling of formaldehyde and formic acid, respectively, with methanol. Consistent with this reasoning, the rates of DMM and MF formation increase with oxygen partial pressure. DMC is formed by carbonylation of methanol, and the rate of its formation increases with CO partial pressure. Increasing methanol partial pressure has an equivalent effect on the rates of DMM and DMC formation, suggesting that both products are formed from a common precursor derived from methanol, for example a methoxide group.

Keywords: Dimethyl carbonate; Dimethoxy methane; Cu-ZSM-5

1. Introduction

Dimethyl carbonate (DMC) can be used as a fuel additive to replace methyl tert-butyl ether (MTBE) [1], a precursor for synthesis of carbonic acid derivatives [2], as a methylating agent to replace methyl halides and dimethyl sulfate, and as an intermediate in the synthesis of polycarbonates and isocyanates [2,3]. Whereas DMC has been made from methanol and phosgene, there has been considerable interest in exploring more environmentally benign processes for this product, such as the oxidative carbonylation of methanol; carbonylation of methylnitrite, ethylenecarbonate, or urea transesterification; direct synthesis from CO_2; alkylation of metal carbonates with organic halides; and decarbonylation of dimethyl oxalate [4]. Of these alternatives, the most promising route is the vapor-phase oxidative carbonylation of methanol, $2CH_3OH + CO + \frac{1}{2}O_2 \rightarrow (CH_3O)_2CO + H_2O$ [5].

A number of copper-based catalysts have been investigated for the vapor-phase oxidative carbonylation of methanol [6–22]. These include CuCl and $CuCl_2$ supported on activated carbon [6–12]; CuCl, $CuCl_2$, and bimetallic $PdCl_2$-$CuCl_2$ deposited on mesoporous silica supports (HMS silica, MCM-41, and SBA-15) [14–16]; and Cu/silica [23]. There have also been reports that the activity and selectivity of the above-mentioned catalysts can be increased by the incorporation of quaternary ammonium salts such as tetrabutylammonium bromide (TBAB) and tetraelthylammonium chloride (TEAC) [16,17]. Because chloride-containing catalysts can lead to reactor corrosion, several authors have examined the potential of copper-exchanged zeolites as catalysts [19,20,24,25]. King [20] have reported that Cu-Y zeolite exhibits good activity and selectivity for DMC synthesis with little catalyst deactivation. Under similar conditions, zeolites exchanged with cuprous cations were found to have higher activity and higher selectivity than catalysts based on cuprous chloride. More recently, Root et al. [19] compared the performance of Cu-X and Cu-ZSM-5, and reported that Cu-X exhibited higher selectivity. In situ infrared studies revealed that CO is more strongly adsorbed on Cu cations ex-

* Corresponding author. Fax: +1 510 642 4778.
E-mail address: bell@cchem.berkeley.edu (A.T. Bell).

0021-9517/$ – see front matter
doi:10.1016/j.jcat.2006.09.002

changed into ZSM-5 than X zeolite. The authors proposed that the synthesis of DMC proceeds via an Eley-Rideal process in which gas-phase CO reacts with the methoxide species bonded to the Cu cations present in the zeolite, and that strong adsorption of CO inhibits the adsorption of methanol, which is required to form methoxide species. Recent work by Drake et al. [24] on Cu-exchanged Y zeolite revealed that all of the Cu exchanged is present as Cu^+ in sites I′, II, and III′. In addition to DMC, this catalyst was found to produce dimethoxy methane (DMM) and methyl formate (MF). In situ infrared and XANES showed that both methoxide and carbonyl groups are associated with the Cu^+ cations of the zeolite, in agreement earlier reports of Root and Anderson for Cu-X [19]. Preliminary work by the present authors using well-characterized Cu-ZSM-5 [25] revealed that this catalyst also produces DMC, DMM, and MF; however, in contrast to Cu-Y, the selectivity of DMM is higher than that of DMC. The present work was undertaken with an aim of understanding in greater detail the effects of reaction conditions on the distribution of products. In situ XANES and infrared spectroscopy were used to characterize the oxidation state of Cu cations in the zeolite and the nature of species associated with these cations.

2. Experimental

2.1. Catalyst preparation and characterization

Cu-exchanged ZSM-5 was prepared via solid-state ion exchange (SSIE) of H-ZSM-5 and CuCl at 1023 K, as described previously [25]. Freshly prepared catalyst was stored in a dry-box before use. The oxidation state of Cu in Cu-ZSM-5 was determined by Cu K-edge X-ray absorption near-edge analysis (XANES), which was carried out in transmission mode at the Stanford Synchrotron Radiation Laboratory (SSRL) on beamline 2–3. This beamline is equipped with a double-crystal monochromator, Si(111), detuned to 70% intensity to minimize the presence of higher harmonics. The samples were pressed into self-supporting wafers (calculated to have an absorbance of 2.5) and then mounted in a controlled-atmosphere cell operated at 101 kPa. After characterization by XAS, each sample was cooled to 298 K before being exposed to a particular gas or gas mixture. In separate experiments, pretreated Cu-ZSM-5 was exposed to a mixture of He/CH_3OH, He/CO, $He/CO/O_2/CH_3OH$, or He/O_2. Methanol vapor was introduced using a gas saturator containing liquid methanol at 298 K. To examine the effects of gas adsorption, the sample was exposed to a flow of gas at room temperature, and the temperature was then raised at a rate of 10 K min^{-1} to 403 K and held at this level for 1 h. All XAS measurements were made in situ. Cu XANES data were analyzed with the IFEFFIT package [26]. Pre-edge absorptions due to the background and detector were subtracted using a linear fit to the data in the range −200–50 eV relative to the sample edge energy (E_0). Each spectrum was normalized by a constant determined by the average absorption in the range 100–300 eV relative to E_0. The edge energy of each sample and reference was taken at the first inflection point beyond any pre-edge peaks.

2.2. Measurement of catalyst activity and selectivity

Measurements of catalyst activity and selectivity were carried out using 150 mg of catalyst loaded into a 10-mm i.d. tubular flow reactor made of quartz. Before exposure to reactants, the catalyst was pretreated at 873 K for 1 h in a stream of high-purity He (99.999%). For the catalytic experiment, a CO/O_2 mixture (25.0% CO, 2.5% O_2, balance He) and He (99.999%) were used. Methanol (CH_3OH) was introduced by passing the CO/O_2 mixture through a saturator maintained at a constant temperature of 293 K. A $CH_3OH/O_2/CO/He$ mixture (4.0/1.0/9.0/19.3) was fed to the reactor at a nominal total flow rate of 20 cm^3/min and was varied between 3 and 80 cm^3/min to study the effect of residence time on product distribution at 403 K. A second experiment designed to study the effect of temperature on the oxidative carbonylation of methanol was carried out using a fresh sample of Cu-ZSM-5. For this study, a $CH_3OH/O_2/CO/He$ mixture (4.0/1.0/9.0/19.3) was fed to the reactor at a nominal total flow rate of 20 cm^3/min, and the reactor temperature was increased from 298 to 423 K. Studies of methanol oxidation in the absence of CO were also carried out. For these experiments, a $CH_3OH/O_2/He$ mixture (4.0/1.0/28.3) was fed to the reactor at a nominal total flow rate of 20 cm^3/min and was varied between 3 and 80 cm^3/min to study the effect of residence time on product distribution at 403 K.

2.3. Infrared characterization of adsorbed species

Infrared spectra were recorded on a Nicolet Nexus 670 FTIR spectrometer equipped with an MCT-A detector. Measurements were taken using a resolution of 4 cm^{-1}. The catalyst were pressed into 20-mg self-supporting pellets and then placed into an infrared cell equipped with CaF_2 windows. Before adsorbate exposure, the catalyst was heated in He at 673 K. Either 16 or 32 scans were averaged to obtain each spectrum.

3. Results

3.1. Characterization of Cu-ZSM-5

Fig. 1 illustrates the IR spectrum for the O–H stretching region. Spectra are shown for H-ZSM-5 and Cu-ZSM-5. The intensity of the band at 3610 cm^{-1}, which is characteristic of Brønsted acid protons [27], approached zero for Cu-ZSM-5, indicating that exchange via the reaction $ZH + CuCl \rightarrow ZCu + HCl$ was nearly complete. In contrast, the IR peak at 3740 cm^{-1}, which is characteristic of Si–OH groups [27], remained essentially unaltered during the course of cation exchange with CuCl, indicating that Si–OH groups did not undergo SSIE.

Cu K-edge XANES of Cu-ZSM-5 and reference compounds (CuCl, Cu_2O, and CuO) are shown in Fig. 2a; with the corresponding derivative curves given in Fig. 2b. The features in the near-edge region are very sensitive to the changes in the oxidation state and coordination environment of Cu. Cu^{2+} (CuO) exhibits three features in the XANES region: a weak absorption

at about 8975–8979 eV, attributed to the dipole-forbidden 1s–3d electronic transition; a shoulder at 8986.7 eV due to a 1s–4p transition; and a very intense peak at 8998 eV [28]. Cu_2O exhibits a well-defined pre-edge peak at 8982.8 eV and a peak maximum at 8996.7 eV. The pre-edge peak lies in an energy range (8982–8985 eV) that is characteristic of 1s–$4p_{xy}$ transitions of Cu(I) in low-coordination environments [29]. CuCl shows a shoulder at 8984.6 eV and a very intense peak at 8987.3 eV. A single, well-defined peak at 8983.6 eV is observed for Cu-ZSM-5. This feature has been assigned to the degenerate 1s–$4p_{x,y}$ electron transition of Cu^+ cations, which are doubly or triply coordinated in a linear or planar configuration, respectively [30,31]. The absence of Cu^{2+} and Cu^0 features rules out the presence of CuO or Cu metal species in copper-exchanged samples. The absence of a peak at 8987.3 eV in the XANES region also suggests the absence of any bulk CuCl.

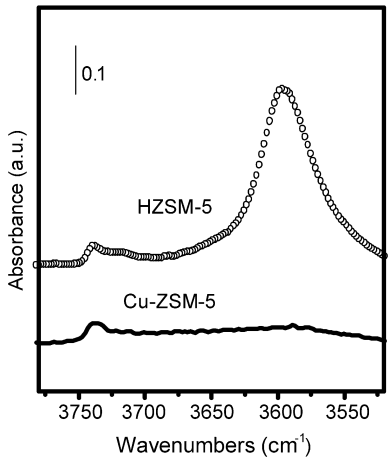

Fig. 1. IR spectra of Cu-ZSM-5 and H-ZSM-5.

3.2. Interaction of CO and Cu cations in Cu-ZSM-5

After the wafer of Cu-ZSM-5 was treated in pure He at 673 K for 30 min and cooled to 298 K, 5.05 kPa of CO was introduced in a He stream and allowed to flow for 10 min. The cell was then purged with He flowing at 40 cm^3/min as the temperature was increased from 298 to 673 K. Fig. 3a shows the IR spectra adsorbed CO. At 298 K, two prominent bands appeared at 2177 and 2151 cm^{-1}, which are assigned to the symmetric and asymmetric stretching modes of the dicarbonyl complex, respectively [32]. However, the existence of monocarbonyl species $[Cu(CO)]^+$ cannot be excluded. The latter species exhibit a band at 2157 cm^{-1} [33] and may be embedded in the broad band for the dicarbonyls. When the temperature was increased from 298 to 373 K, the band at 2177 cm^{-1} disappeared and the band at 2151 cm^{-1} appeared to shift to 2157 cm^{-1}. This pattern is attributed to desorption of CO from the dicarbonyl species, so that only the more strongly bound monocarbonyl species remained. With further increases in temperature, the intensity of the band for monocarbonyl species decreased. However, the stretching band of a monocarbonyl complex can still be observed even at temperatures above 673 K, indicating that the interaction of CO with Cu cations in ZSM-5 is quite strong.

Previous studies of CO adsorption on Cu-ZSM-5 have reported the presence of two strongly adsorbed forms of CO showing bands at 2159 and 2155 cm^{-1} [34]. These bands were assigned to linearly adsorbed CO associated with Cu^+ cations coordinated to two- and three-zeolite lattice O atoms. CO adsorbed on di-coordinated Cu^+ cation was estimated to have a heat of adsorption of 121.4 kJ/mol, whereas CO adsorbed on tri-coordinated Cu^+ was estimated to have a heat of adsorption of 100.5 kJ/mol. Recent DFT calculations by Davidová

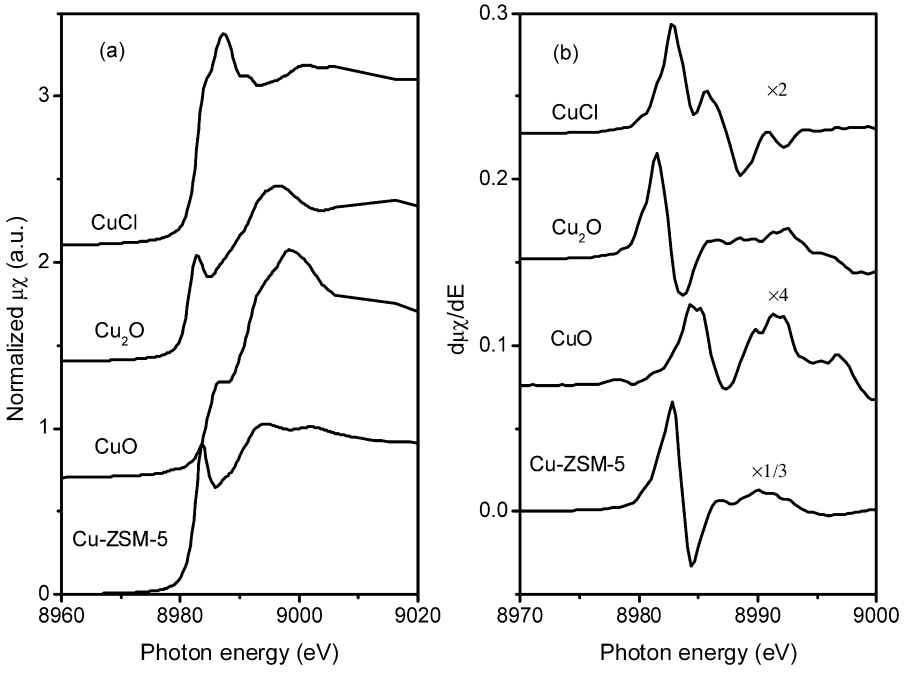

Fig. 2. Cu K-edge XANES of standards and Cu-ZSM-5 (a) and the corresponding derivative curves (b).

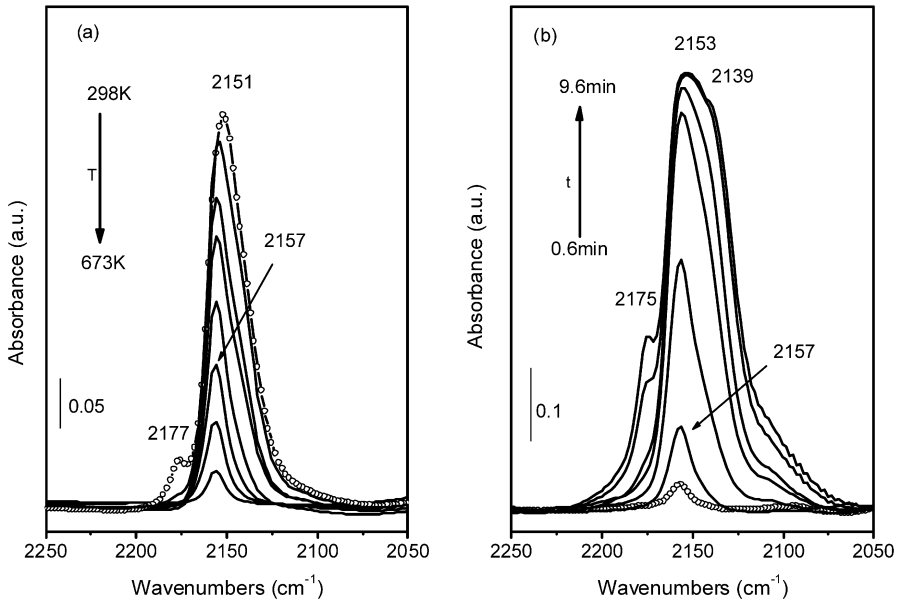

Fig. 3. IR spectra of Cu-ZSM-5 (a) CO desorption as a function of temperature (pre-adsorbed CO at 5.05 kPa for 15 min, then purge with a He flow of 40 ml/min at a T ramp: 5 K/min) and CO adsorption at 403 K as a function of time (b) (feed flow: 20 ml/min; CO pressure: 20.2 kPa; balanced by He).

et al. [35] support these assignments. Those authors calculated a heat of adsorption of 146.9 kJ/mol for CO adsorbed on Cu^+ cations situated at II(I2) sites in which Cu^+ is coordinated with two O atoms of an AlO_4 tetrahedron located at the intersection of two channels in the MFI structure. The calculated a heat of adsorption of 119.7 kJ/mol for CO adsorbed on Cu^+ cations situated at I(Z6) sites in which Cu^+ is coordinated to three or four O atoms within a six-membered aluminosilicate ring located on the wall of one of the channels.

The IR spectrum of CO adsorbed on Cu-ZSM-5 was also recorded at 403 K with a CO partial pressure of 20.2 kPa. As shown in Fig. 3b, on introduction of CO, a band appeared instantaneously at 2157 cm^{-1}. With prolonged contact time, this band shifted to 2153 cm^{-1}, and a new band appeared at 2175 cm^{-1}, as did a shoulder at 2139 cm^{-1}. The band at 2157 cm^{-1} is attributed to the formation of monocarbonyl species, whereas the bands at 2175 and 2153 cm^{-1} are attributed to dicarbonyl species. The absorption at 2139 cm^{-1} has been attributed to CO molecules interacting weakly with the zeolite framework through van der Waals forces [36].

3.3. Interaction of CH_3OH with Cu-ZSM-5

Figs. 4a and 4b show IR bands observed when Cu-ZSM-5 was exposed to methanol at 403 K. Well-defined bands are observed at 2953, 2843, 1461, and 1353 cm^{-1}. The bands at 2953 and 2843 cm^{-1} shown in Fig. 4a are due to the antisymmetric and symmetric C–H stretching vibrations, respectively, of molecularly adsorbed methanol, whereas the bands at 1461 and 1353 cm^{-1} are characteristic of bending vibrations for molecularly adsorbed methanol [37]. The two bands for C–H stretching vibrations shown in Fig. 4a are similar to those reported by King at 2955 and 2847 cm^{-1} for molecularly adsorbed methanol adsorbed Cu-Y at 403 K [21]. Weak features at 2932 and 2826 cm^{-1} are also shown in Fig. 4a; these are likely due

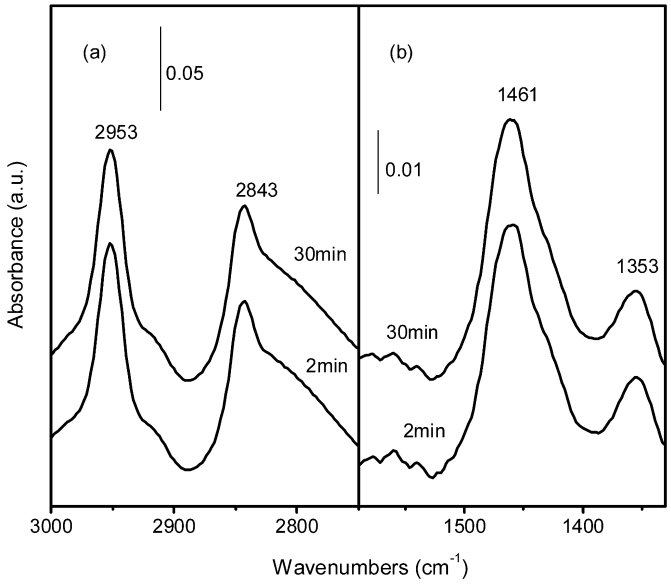

Fig. 4. Infrared spectra of methanol adsorption on Cu-ZSM-5 at 403 K (feed flow: 20 ml/min; CH_3OH pressure: 12.12 kPa).

to methoxide species [21]. Drake et al. also observed evidence of both molecularly adsorbed methanol and methoxide species during the synthesis of DMC over Cu-Y [24].

3.4. Interaction of $CH_3OH/CO/O_2$ with Cu-ZSM-5

Fig. 5 shows IR spectra taken during exposure of Cu-ZSM-5 to a $MeOH/CO/O_2/He$ mixture (12.12/20.2/2.02/66.66 kPa) at 403 K. Before introduction of the gas mixture, the catalyst was exposed to a CO/He mixture (20.2/80.8 kPa) at 403 K. With time under reaction conditions, the intensities of the C–H stretching vibrations for molecularly adsorbed CH_3OH (2951 and 2844 cm^{-1}) increased in intensity, and two new bands

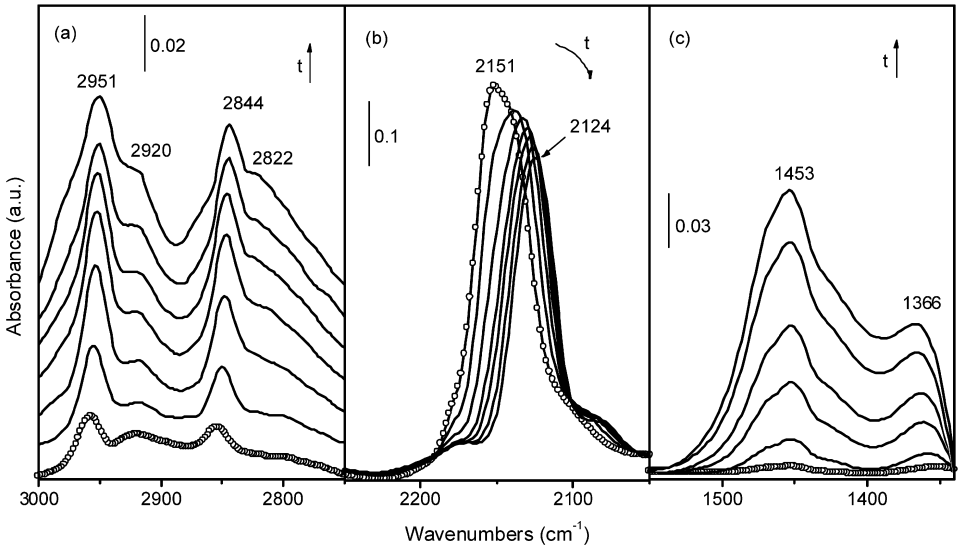

Fig. 5. Infrared spectra of Cu-ZSM-5 under DMC reaction condition as a function of time in stream (feed flow: 20 ml/min, $CH_3OH:CO:O_2 = 12.12:20.2:2.02$ kPa; t: 0.2–2 min).

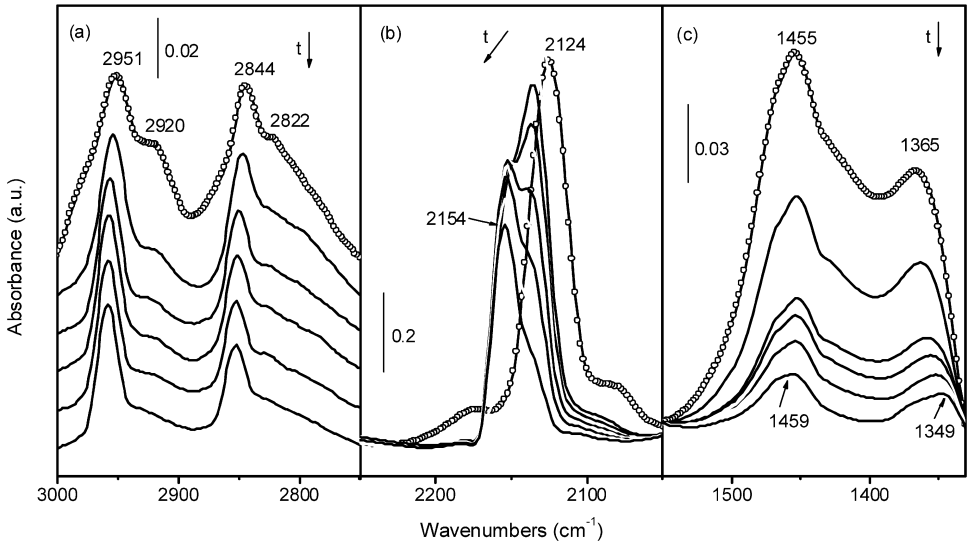

Fig. 6. Infrared spectra of Cu-ZSM-5 after DMC reaction purged in He as a function of time (He flow: 40 ml/min, t: 1–90 min).

appeared at 2920 and 2822 cm^{-1} attributable to methoxide species [21]. The band for adsorbed CO seen at 2151 cm^{-1} before the introduction of MeOH and O_2 to the gas stream diminished in intensity and shifted to 2124 cm^{-1} with increasing time of exposure to the synthesis gas mixture. The latter band is attributed to Cu^+ sites associated with $HOCH_3$ and CO, that is, $[Cu(HOCH_3)(CO)]^+$. The decrease in C–O stretching frequency of CO is ascribed to the enhanced d–π back-donation between Cu^+ and CO when $HOCH_3$ is coordinated to Cu^+. The bands at 1453 and 1366 cm^{-1} are attributed to a combination of methoxide, $[Cu(HOCH_3)(CO)]^+$, and molecularly adsorbed methanol [24].

Fig. 6 shows the IR spectra of Cu-ZSM-5 purged in He after exposure to a mixture of $CH_3OH/CO/O_2$. The bands at 2920 and 2822 cm^{-1} assigned to C–H stretching vibrations of methoxide groups disappeared after 90 min, whereas the bands due to molecularly adsorbed CH_3OH decreased much more slowly. The rapid decay of methoxide species may due to carbonylation by desorbed CO to form DMC. With increasing time under He, the position of the CO band shifted to 2154 cm^{-1} and the intensity of this band became significantly lower than that observed prior to the introduction of CH_3OH and O_2 (see Fig. 5). The blue shift of the CO band is caused by desorption of CH_3OH adsorbed at Cu^+ sites on which CO is also adsorbed. The desorption of methanol and the consumption of methoxide species led to a rapid decrease in the intensity of the bands at 1453 and 1366 cm^{-1} and their shift to 1459 and 1349 cm^{-1}, respectively. This suggests that at the end of He flushing, only molecularly adsorbed methanol associated with Cu^+ sites remained on the catalyst. In agreement with this interpretation, it is observed that the bands at 1461 and 1353 cm^{-1} are attributable to molecularly adsorbed methanol (see Fig. 4b for comparison). The changes in the IR spectra presented in Figs. 5 and 6 suggest that methanol displaces adsorbed CO on some of

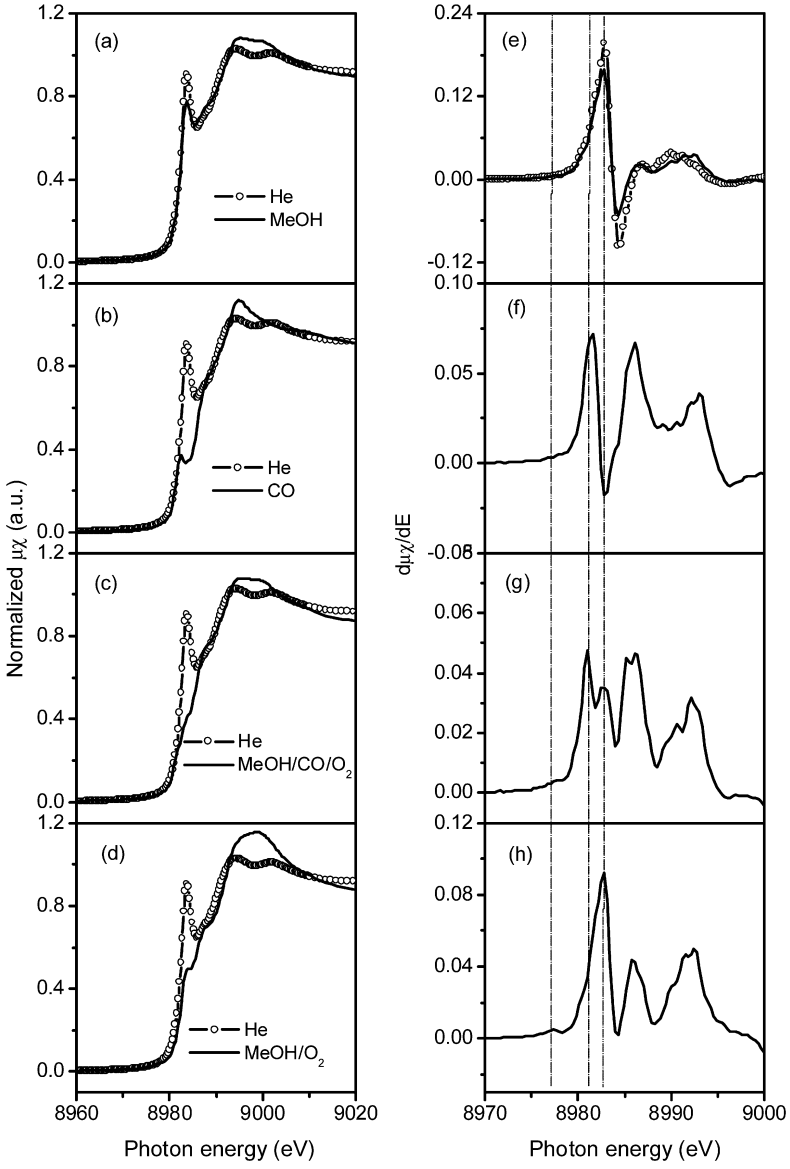

Fig. 7. XANES of Cu-ZSM-5 with contact of different reactants at 403 K (a)–(d) and their corresponding derivative curves (e)–(h).

the Cu^+ sites and coadsorbs with CO on other Cu^+ sites. This pattern is similar to that reported previously for Cu-Y [19,24].

3.5. Cu oxidation state and coordination environment in Cu-ZSM-5 during DMC synthesis

The oxidation state and coordination of Cu was probed by Cu *K*-edge XANES. As shown in Fig. 7, when the catalyst was exposed to CH_3OH at 403 K, the pre-edge peak of Cu^+ remained at the position observed under He but slightly decreased in intensity. Likewise, no significant changes occurred in the corresponding first derivative curve (Fig. 7). This suggests that the molecular adsorption of CH_3OH on Cu^+ sites does not affect the oxidation state of Cu or its coordination to the zeolite framework.

When on He-treated Cu-ZSM-5 was exposed to 20.2 kPa of CO at 403 K, the large resonant peak at 8983.6 eV associated with coordinatively unsaturated Cu^+ was replaced by a shoulder at 8982.4 eV. In the first derivative spectrum, the original peak at 8982.7 eV shown in He and/or MeOH treated samples disappeared completely and was replaced by three new features at 8981.5, 8986.1, and 8993.1 eV. The pre-edge peak had a red shift of 1.2 eV, in good agreement with the value reported by Lamberti et al. [38], who attributed this shift to the formation of dicarbonyl complexes. Kumashiro et al. [34] observed similar effects of CO adsorption on the XANES spectrum of Cu-ZSM-5, which they attributed to a change in the coordination structure of Cu^+ cations.

The first derivative spectrum for Cu-ZSM-5 exposed to a $CH_3OH/CO/O_2$ mixture (12.12/20.2/2.02 kPa) at 403 K (Fig. 7g) showed two well-defined peaks at 8981.5 and 8982.7 eV. The positions of these two features were identical to those observed when CO or CH_3OH, respectively, are adsorbed on Cu^+ cations separately (see above). Taken together with the IR spectra shown in Fig. 5, the XANES data suggest that on exposure of Cu-ZSM-5 containing pre-adsorbed CO to a

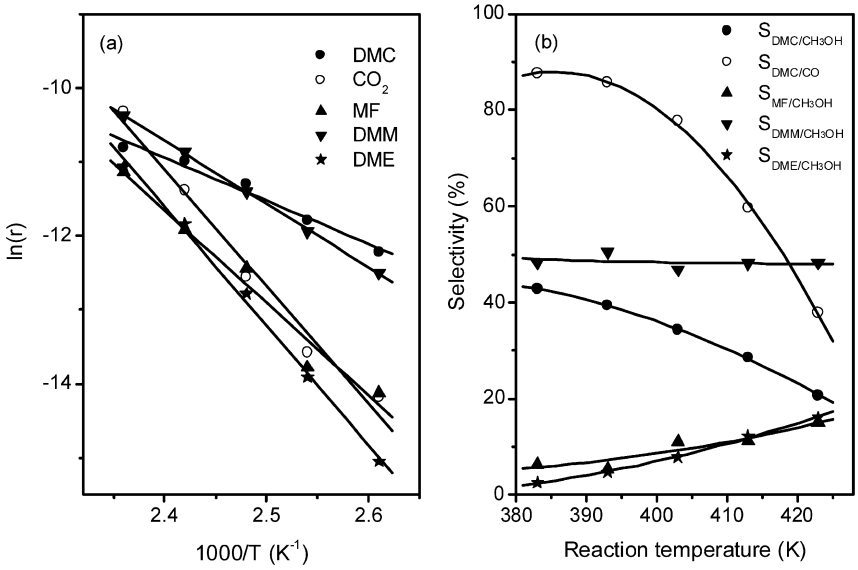

Fig. 8. Effects of reaction temperature on (a) the rates of product formation and (b) product selectivity. Feed—CH_3OH(12.12 kPa)/CO(20.2 kPa)/O_2(2.02 kPa). [$S_{DMC/CO}$ = [DMC]/([DMC] + [CO_2]), $S_{i/CH_3OH} = n[i]/(2[DMC] + 2[MF] + 3[DMM] + 2[DME])$, i: DMC, MF, DMM, DME].

$CH_3OH/CO/O_2$ mixture, the CO was displaced by CH_3OH from a fraction of the Cu^+ cations. The IR data presented in Fig. 5 suggest that both CO and CH_3OH were co-adsorbed on the balance of the Cu^+ cations.

The first derivative XANES spectrum after exposure of Cu-ZSM-5 to a CH_3OH/O_2 mixture (12.12/2.02 kPa), presented in Fig. 7h, exhibits a peak at 8982.7 eV similar to that seen when the catalyst was exposed to CH_3OH alone (Fig. 7e). A small but well-defined peak was also observed at 8977.4 eV, attributed to the presence of Cu^{2+} cations. Several peaks also appeared in the region above 8985 eV. Although the positions of these features were similar to those seen in the spectra of Cu^{2+}-containing reference compounds (see Fig. 2), their presence does not provide definitive evidence for the oxidation of Cu^+ to Cu^{2+}, for the reasons discussed above.

3.6. Catalytic activity and selectivity of Cu-ZSM-5 for DMC and DMM synthesis

Figs. 8a and 8b show the dependence of the rate of product formation and product selectivity, respectively, on the reaction temperature for a fixed feed composition and space velocity. Over the temperature range investigated (383–425 K), the methanol conversion increased from 0.25 to 2.5% and thus was differential under all conditions. The products derived from methanol included DMC, DMM, MF, and DME. Separate experiments conducted without CO in the feed established that no DMC and very little CO_2 were formed via oxidation of methanol. For this reason, the CO selectivity was based purely on the formation of DMC and CO_2. Fig. 8a shows that the rate of formation of each carbon-containing product followed an Arrhenius behavior. The apparent activation energy for each product is listed in Table 1. Fig. 8b shows that at 383 K, the principal products derived from methanol were DMM and DMC in nearly equivalent proportions, with only very small amounts of MF and DME. The selectivity of CO conversion to DMC at 383 K was nearly 90%, with the balance of the CO being CO_2. With increasing temperature, the DMM selectivity remained nearly constant, but the DMC selectivity decreased and the MF and DME selectivities increased. The selectivity of CO to DMC decreased sharply with increasing temperature, and, correspondingly, the selectivity to CO_2 increased.

Table 1
Apparent activation energies for products on Cu-ZSM-5

	DMC	MF	DMM	DME	CO_2
E_{app} (kJ/mol)	49	105	71	135	132

The influence of methanol conversion on product formation rates and selectivities are presented in Figs. 9a and 9b for the case of a $CH_3OH/CO/O_2$ feed mixture and in Figs. 9c and 9d for the case of a CH_3OH/O_2 feed mixture. The concentrations of CH_3OH and O_2 in both feed mixtures are identical. Fig. 9a shows that the rate of DMC formation decreased rapidly with increasing methanol conversion. The rates of DMM and MF formation also dropped off with increasing methanol conversion, but at a lower rate. In contrast, the rates of CO_2 and DME formation passed through a maximum with methanol conversion. The product selectivities also changed dramatically with methanol conversion, as shown in Fig. 9b. The DMC selectivity decreased, whereas DME and MF selectivities increased, and the selectivity to DMM passed through a maximum.

Figs. 10a, 10b, and 10c show the effects of CO, CH_3OH, and O_2 pressure on the rates of DMC, MF, DMM, DME, and CO_2 formation. With increasing CO pressure, the rate of DMC formation increased, whereas the rates of DMM and MF formation decreased. The rates of DME and CO_2 formation increased slightly with the initial increase in CO partial pressure and then either decreased slightly or remained nearly constant with further increases in CO partial pressure. Increasing the methanol partial pressure caused a small increase in the rates of DMM and DMC formation, both of which remained nearly

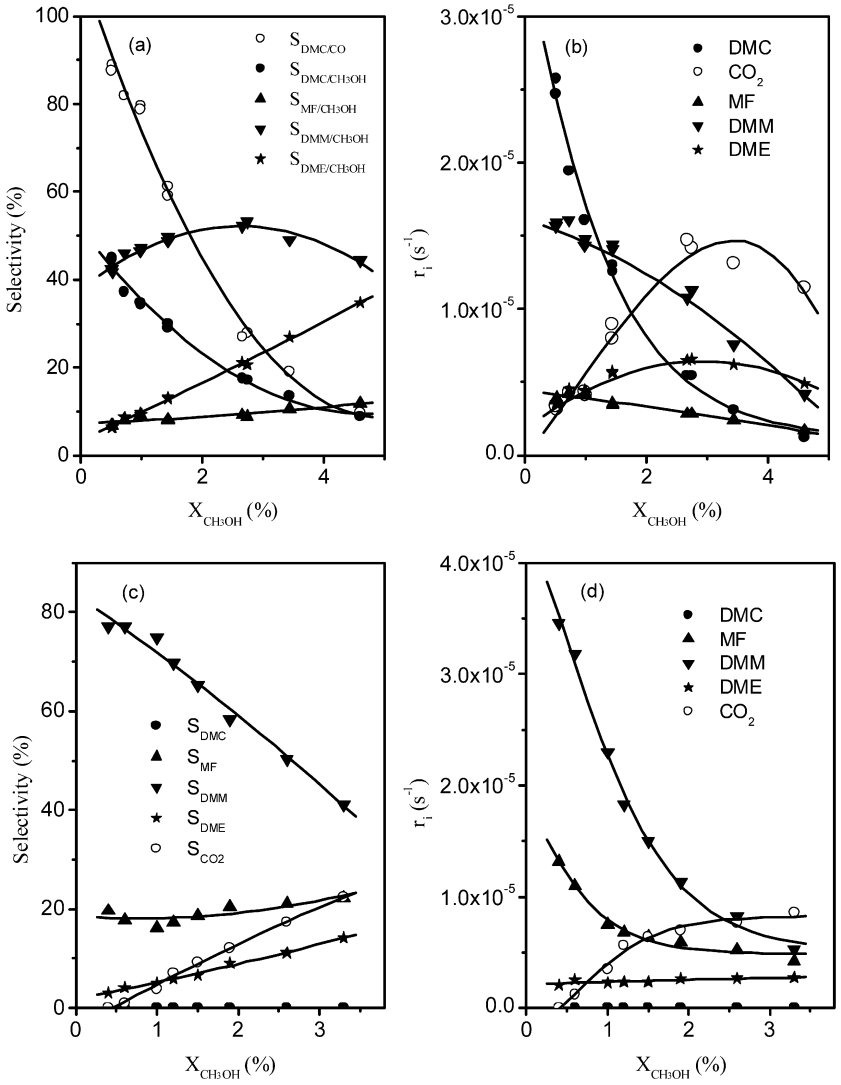

Fig. 9. Selectivities and production rates as a function of methanol conversion by varying the residence time on Cu-ZSM-5 at 403 K under $CH_3OH/CO/O_2$ (12.12/20.2/2.02 kPa) (a, b) [$S_{DMC/CO} = [DMC]/([DMC] + [CO_2])$, $S_{i/CH_3OH} = n[i]/(2[DMC] + 2[MF] + 3[DMM] + 2[DME])$, i: DMC, MF, DMM, DME] and CH_3OH/O_2 (12.12/2.02 kPa) (c, d) [$S_{i/CH_3OH} = n[i]/(2[DMC] + 2[MF] + 3[DMM] + 2[DME] + [CO_2])$, i: DMC, MF, DMM, DME, CO_2].

equivalent. The rates of MF, DME, and CO_2 formation were all nearly equivalent and decreased slightly with increasing methanol partial pressure. The rates of DMM, DMC, and MF formation increased with increasing O_2 partial pressure, and above an O_2 partial pressure of 2.53 kPa, the rate of DMM formation became larger than that of DMC formation. The rates of DME and CO_2 formation were almost equivalent and showed an initial increase, then leveled off as the partial pressure of oxygen increases. On the other hand, the rate of MF formation exhibited a monotonic increase with increasing O_2 partial pressure. Apparent reaction orders in CO, O_2, and CH_3OH for the formation of DMC, DMM, and MF are given in Table 2.

4. Discussion

Solid-state exchange of H-ZSM-5 with CuCl at 1023 K led to virtually complete substitution of the Brønsted acid protons of the zeolite by Cu^+ cations. This conclusion is supported by the absence of the IR band at 3610 cm^{-1} for vibrations of Brønsted acid protons and the presence of a Cu K-edge XANES spectrum characteristic of Cu^+. No evidence was found in the XANES spectrum of Cu^{2+} in the as-prepared catalyst. When Cu-ZSM-5 was exposed to a CH_3OH/O_2 mixture at 403 K, a small peak appeared at 8977.4 eV characteristic of Cu^{2+}, but most of the spectrum was still representative of Cu^+. When CO was added to this feed mixture, the feature characteristic of Cu^+ in the derivative XANES spectrum split into two parts, one characteristic of CO adsorbed on Cu^+ and the other characteristic of CH_3OH adsorbed on Cu^+. In situ IR spectra during the exposure of the catalyst to a $CH_3OH/CO/O_2$ mixture at 403 K showed features for molecularly adsorbed CH_3OH and CO, and for OCH_3 species. The position of the CO band suggests that CO and $HOCH_3$ may be coadsorbed on the same Cu^+ cation. Because the removal of methoxide species in He flow (Fig. 6) resulted in the reappearance of the band for CO at 2154 cm^{-1}, the coadsorption of CO and $HOCH_3$ groups is believed to occur on the type II(I2) sites. This then suggests that methanol adsorp-

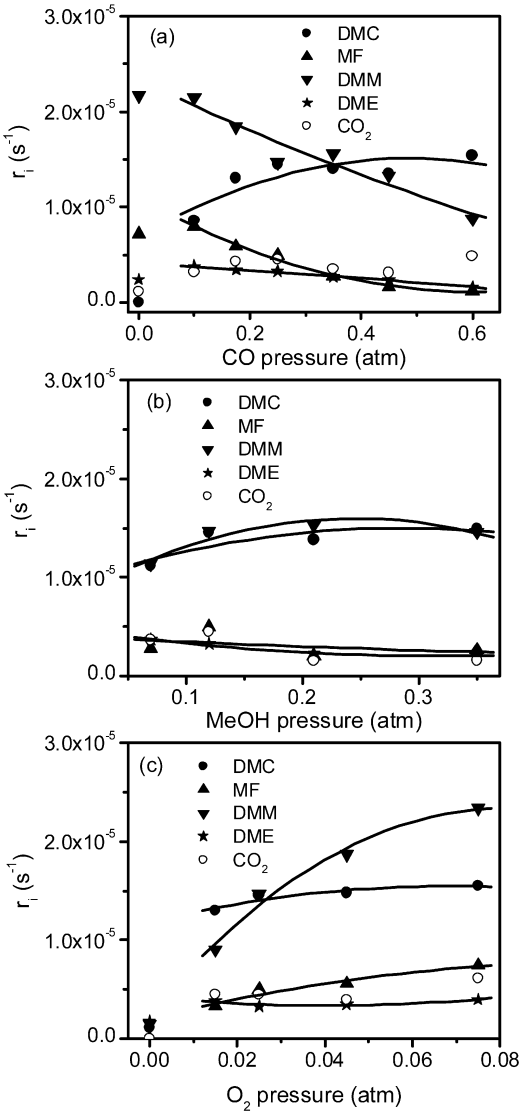

Fig. 10. Effect of reactant pressure on oxidative carbonylation of methanol at 403 K: (a) CO (CH_3OH: 12.12 kPa; O_2: 2.53 kPa); (b) CH_3OH (CO: 25.25 kPa, O_2: 2.53 kPa); (c) O_2 (CO: 25.25 kPa, CH_3OH: 12.12 kPa).

tion resulted in complete displacement of CO adsorbed on type I(M6) sites, on which CO is more weakly bound [33,34].

Table 3 compares the activity of Cu-ZSM-5 reported in this study with that reported by Anderson and Root [19] for essentially comparable reaction conditions. It is evident that both samples of ZSM-5 exhibited comparable turnover frequencies for DMC synthesis. Table 3 also demonstrates that the rate of DMC synthesis observed over Cu-ZSM-5 is on the same order of magnitude as that reported previously for Cu-X [18], Cu-Y [20], Cu/SBA [23], Cu/MCM-41 [15], and CuCl/AC [9]. What is notable, however, is that the methanol selectivity to DMC was significantly lower on Cu-ZSM-5 than on all other catalysts, and that the DMM selectivity was correspondingly higher. This difference is hard to explain, because recent XAS studies of Cu-Y and Cu-ZSM-5 prepared by SSIE demonstrate that in both cases all of the Cu is present as Cu^+ in cation-exchange positions [24,25]. But subtle differences are observed when XAS is carried out under reaction conditions. CO appears to be more strongly adsorbed relative to CH_3OH on Cu-ZSM-5 compared with Cu-Y [19,24]. The relationship between the coadsorption of CO and CH_3OH and the synthesis of DMC remains unclear, as does the issue of what dictates the selectivity between the synthesis of DMM and DMC. Root and coworkers [19] have suggested that DMC synthesis occurs only on Cu^+ sites devoid of adsorbed CO, because Cu-X exhibits a higher turnover frequency for DMC synthesis and a weaker strength of CO adsorption than Cu-ZSM-5. However, this interpretation would not explain why the DMM selectivity is higher on Cu-ZSM-5 (see Table 3). Consequently, the search for an explanation of the effect of zeolite structure and Si/Al ratio remains a subject of ongoing research.

A detailed mechanism by which DMC, DMM, and, MF—the primary products derived from methanol—cannot be developed based on the information presented here. Nevertheless, some inferences can be drawn regarding the pathways by which methanol is converted to these products and how they are then converted to secondary products, DME and CO_2. Scheme 1 illustrates the proposed relationships between the reactants, CH_3OH, CO, and O_2, and both the primary and secondary products. In the absence of CO, CH_3OH can undergo sequential oxidation to CH_2O, HCOOH, and CO_2. The results

Table 2
Reaction orders for the formation of DMC, DMM, MF, and DME

Reaction orders	DMC	DMM	MF	DME
CO	0.4	−0.3	−0.7	−0.2
O_2	0.2	0.5	0.5	0
CH_3OH	0.2	0.2	−0.2	−0.4

Table 3
Summary of DMC synthesis on different Cu based catalysts

Catalyst	Cu content (wt%)	Reaction temperature (K)	CO (kPa)	O_2 (kPa)	MeOH (kPa)	TOF_{DMC} ($s^{-1} \times 10^5$)	Sel_{DMC} (%)
CuCl/SBA[23]	2.9	403	27.3	3.0	12.1	3.5	80.1
$CuCl_2$/AC[9]	4.6	393	767.6	50.5	191.9	3.1	80.2
CuCl/MCM-41[15]	6.3	403	444.4	50.5	30.3	0.85	100
Cu/X[18]	30	403	40.4	8.1	20.2	2	–
Cu/Y[20]	7.3	403	46.5	6.1	26.3	6.8	80
Cu/ZSM-5[19]	7	403	30.3	8.1	20.2	1.4	–
Cu/Y[24]	23.5	403	20.2	2.0	12.1	2.8	70

Note. TOF reported on a total Cu basis. Where appropriate, the reported TOF valve was converted to common units based on details in Section 2 of the listed reference.

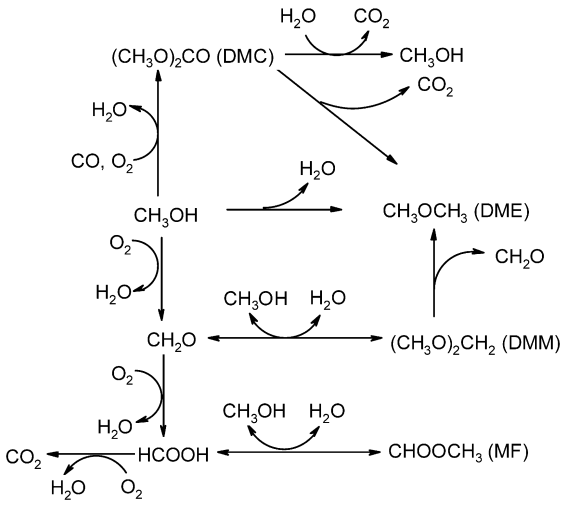

Scheme 1.

shown in Fig. 9c suggest that at 403 K, the oxidation of CH_3OH did not lead to CO_2, because CO_2 was not observed in the limit of very low methanol conversion. Although CH_2O and HCOOH were not observed in the reactor effluent, the formation of these products can be inferred, because both DMM and MF, the products of CH_3OH reaction with these intermediates, were observed as primary products. The appearance of CO_2 with increasing methanol conversion can be attributed to the decomposition of DMM to DME and CH_2O, followed by oxidation to HCOOH and then to CO_2 and H_2O. Additional CH_2O may form as a result of the hydrolysis of DMM and MF, as shown in Scheme 1.

With increasing addition of CO to the CH_3OH/O_2 feed mixture, the rates of DMM and MF formation decreased as the rate of DMM formation increased (see Fig. 10a). As shown in Scheme 1, this trend suggests that the oxidative carbonylation of methanol to DMC competes favorably with the oxidation of methanol to DMM. The monotonic increase in the rate of DMC synthesis with increasing CO partial pressure is similar to that reported previously by Root and Anderson [19] for both Cu-X and Cu-ZSM-5, supporting their conclusion that CO insertion into adsorbed methoxide species is the rate-determining step in DMC synthesis. This conclusion is also supported by the observation of a near zero-order dependence of the rates of DMC and DMM formation on methanol partial pressure shown in Fig. 10b. Fig. 9a shows that as the conversion of methanol approached zero, DMC became the dominant product, followed by DMM and MF in that order. This figure also shows that the rate of CO_2 and DME formation became small. With increasing methanol conversion, the rates of DMC, DMM, and MF formation all decreased, whereas the rates of CO_2 and DME formation increased and passed through a maximum. These trends may be explained by two secondary reactions, as shown in Scheme 1. The first reaction is the decomposition of DMC to DME and CO_2; the second is the hydrolysis of DMC to CO_2 and CH_3OH. The latter reaction is expected to become more important as the conversion of methanol increases, as is shown in Fig. 9. Once the concentration of DMC becomes small enough, the rate of CO_2 formation will fall off, because there is no longer sufficient DMC to contribute to CO_2 formation via either DMC decomposition or hydrolysis.

5. Conclusion

Solid-state exchange of H-ZSM-5 with CuCl vapor at 1023 K leads to complete displacement of Brønsted acid protons by Cu^+ cations. The oxidation of methanol over Cu-ZSM-5 prepared in this manner produces DMM as the primary product, with small amounts of MF and DME. With increasing feed residence time (i.e., decreasing feed flow rate), the rates of DMM and MF decrease, and the rate of CO_2 formation increases. An illustrated in Scheme 1, DMM is believed to be formed via the coupling of formaldehyde (formed by partial oxidation of methanol) with methanol, whereas MF is believed to be formed via coupling of formic acid (produced by the oxidation of formaldehyde) with methanol. In the absence of Brønsted acid protons, DME is thought to be formed via the decomposition of DMM and DMC. When CO is added to the feed stream, the oxidative carbonylation of methanol leads to DMC, and with increasing partial pressure of CO, the rate of DMC formation increases while the rate of DMM formation decreases. In contrast, the rates of DMC and DMM formation increase slightly with increasing methanol partial pressure, and both products are equally sensitive to this variable. This suggests that the formation of DMM and DMC pass through a common intermediate, presumably the methoxide species, which are observed by in situ IR spectroscopy. As might be expected, the rates of DMM and MF formation increase with oxygen partial pressure, but the rate of DMC formation remains relatively insensitive to this variable. The apparent activation energy for the formation of the various products observed increases in the order DMC < DMM < MF < $CO_2 \approx$ DME. As a result, DMC selectivity is highest at low temperatures. In situ IR spectroscopy and XANES show that methanol can adsorb on Cu^+ cations as both molecular CH_3OH and CH_3O, with very little effect on the coordination of the Cu cations to zeolite framework. When CH_3OH, CO, and O_2 are introduced together at reaction temperature, IR spectroscopy provides evidence for the co-adsorption of CO and CH_3O on a single Cu^+ cation, as well as the presence of CO adsorbed alone. With increasing methanol conversion, the decomposition of DMC to DME and CO_2 and the hydrolysis of DMC to CO_2 and CH_3OH contribute to the loss of DMC from the product stream.

Acknowledgments

The authors thank the synchrotron laboratories of SSRL and ALS for the allocated beam time and assistance. This work is supported by the Methane Conversion Cooperative (MC^2) funded by BP.

References

[1] M.A. Pacheco, C.L. Marshall, Energy Fuels 11 (1997) 2.
[2] Y. Ono, Pure Appl. Chem. 68 (1996) 367.

[3] Y. Ono, Appl. Catal. A 155 (1997) 133.
[4] D. Delledonne, F. Rivetti, U. Romano, App. Catal. A 221 (2001) 241.
[5] P. Yang, Y. Cao, W. Dai, J. Deng, K. Fan, Appl. Catal. A 243 (2003) 323.
[6] G.L. Curnutt, A.D. Harley, in: Oxygen Complexes and Oxygen Activation by Transition Metals, Plenum, New York, 1988, pp. 215–232.
[7] G.L. Curnutt, U.S. patent, 4,625,044, 1986.
[8] G.L. Curnutt, U.S. patent, 5,004,827, 1991.
[9] M.S. Han, B.G. Lee, I. Suh, H.S. Kim, B.S. Ahn, S.I. Hong, J. Mol. Catal. A 170 (2001) 225.
[10] M.S. Han, B.G. Lee, I. Suh, B.S. Ahn, H.S. Kim, D.J. Moon, S.I. Hong, J. Mol. Catal. A 203 (2003) 137.
[11] K. Tomishige, T. Sakaihori, S. Sakai, K. Fujimoto, Appl. Catal. A 181 (1999) 95.
[12] H. Itoh, Y. Watanabe, K. Mori, H. Umino, Green Chem. 5 (2003) 558.
[13] R.X. Jiang, S.F. Wang, X.Q. Zhao, Y.J. Wang, C.F. Zhang, Appl. Catal. A 238 (2003) 131.
[14] Y. Cao, J.C. Hu, P. Yang, W.L. Dai, K. Fan, Chem. Commun. (2003) 908.
[15] Z. Li, K. Xie, R.C.T. Slade, Appl. Catal. A 205 (2001) 85.
[16] P. Yang, Y. Cao, J.C. Hu, W.L. Dai, K. Fan, Appl. Catal. A 241 (2003) 363.
[17] D.C. Molzahn, M.E. Jones, G.E. Hartwell, J. Puga, U.S. patent 5,387,708.
[18] S.A. Anderson, T.W. Root, J. Catal. 217 (2003) 396.
[19] S.A. Anderson, T.W. Root, J. Mol. Catal. A 220 (2004) 247.
[20] S.T. King, J. Catal. 161 (1996) 530.
[21] S.T. King, Catal. Today 33 (1997) 173.
[22] S.T. King, M.E. Jones, M.M. Olken, U.S. patent 5,391,803, 1995.
[23] I.J. Drake, K.L. Fujdala, A.T. Bell, T.D. Tilley, J. Catal. 230 (2005) 14.
[24] I.J. Drake, Y. Zhang, D. Briggs, B. Lim, T. Chau, A.T. Bell, J. Phys. Chem. B 110 (2006) 11654.
[25] Y. Zhang, I.J. Drake, A.T. Bell, Chem. Mater. 18 (2006) 2347.
[26] (a) M. Newville, J. Synchrotron Radiat. 8 (2001) 322;
(b) IFEFFIT manual: http://cars9.uchicago.edu/ifeffit/;
(c) B. Ravel, M. Newville, J. Synchrotron Radiat. 12 (2005) 537.
[27] A. Zecchina, S. Bordiga, G. Spoto, D. Scarano, G. Petrini, G. Leofanti, M. Padovan, A.C. Otero, J. Chem. Soc. Faraday Trans. 88 (1992) 22,959.
[28] C. Prestipino, G. Berlier, F.X. Llabres i Xamena, G. Spoto, S. Bordiga, A. Zecchina, G.T. Palomino, T. Yamamoto, C. Lamberti, Chem. Phys. Lett. 363 (2002) 389.
[29] L.-Sh. Kau, D.J. Spira-Solomon, J.E. Penner-Hahn, K.O. Hodgson, E.I. Solomon, J. Am. Chem. Soc. 109 (1987) 6433.
[30] C. Lamberti, S. Bordiga, M. Salvalaggio, G. Spoto, A. Zecchina, F. Geobaldo, G. Vlaic, M. Bellatreccia, J. Phys. Chem. B 101 (1997) 344.
[31] C. Lamberti, S. Bordiga, F. Bonino, C. Prestipino, G. Berlier, L. Capello, F. D'Acapito, F.X. Llabrés i Xamena, A. Zecchina, Phys. Chem. Chem. Phys. 5 (2003) 4502.
[32] S. Bordiga, G.T. Palomino, D. Arduino, C. Lamberti, A. Zecchina, C.O. Arean, J. Mol. Catal. A 146 (1999) 97.
[33] A. Zecchina, S. Bordiga, M. Salvalaggio, G. Spoto, D. Scarano, C. Lamberti, J. Catal. 173 (1998) 540.
[34] R. Kumashiro, Y. Kuroda, M. Nagao, J. Phys. Chem. B 103 (1999) 89.
[35] M. Davidová, D. Nachtigallova, P. Natichgall, J. Phys. Chem. B 108 (2004) 13,674.
[36] V. Gruver, A. Panov, J.J. Fripiat, Langmuir 12 (1996) 2505.
[37] I.A. Fisher, A.T. Bell, J. Catal. 172 (1997) 222.
[38] C. Lamberti, S. Bordiga, F. Bonino, C. Prestipino, G. Berlier, L. Capello, F. D' Acapito, F.X. Llabrés i Xamena, A. Zecchina, Phys. Chem. Chem. Phys. 5 (2003) 4502.